AIAA JOURNAL
Vol. 41, No. 11, November 2003

Thin Airfoil in Fields of Nonuniform Density, Part 2: Low-Density Strip

Frank E. Marble*
California Institute of Technology, Pasadena, California 91125

An analysis that allows the calculation of the loading, lift coefficient, and moment coefficient response of a lightly loaded airfoil as it passes through a strip of gas whose density differs strongly from that of the main stream is developed. Although it builds on the treatment of a lightly loaded airfoil passing through a single plain density interface, it necessitates a quite different analysis and produces some novel results related to the comparative breadth of the strip and the chord of the airfoil and to its inclination with respect to the undisturbed flow direction. The unique characteristics that differentiate the effects of the strip from those of a single interface are examined in detail. The image principle is not applicable when the field contains two or more density interfaces. Instead and not surprisingly, the solution can be represented as an infinite set of images making the result less transparent than those for the single interface. But the image principle proves to offer a considerable advantage in the physical interpretation of the effects of normal and inclined strips. Detailed results of the encounter of a flat-plate airfoil with a strip having a density half that of the freestream are presented for the strips having breadths of 0.4, 0.8, and 1.2 times the airfoil chord and oriented normal to the undisturbed flow direction and at an angle of 60 deg to the undisturbed flow direction. Impulsive loads accompany the passage of each of the two density interfaces over the leading edge and over the trailing edge of the airfoil, and consequently the loading "signature" varies substantially with both breadth and orientation of the strip. For examples where the breadth of the strip is 1.2 times the airfoil chord so that the strip completely covers the airfoil for a portion of its encounter, the results resemble the passage of two independent single interfaces.

Nomenclature

C_L = airfoil lift coefficient
C_{L0} = steady lift coefficient at density ρ_1
C_M = airfoil moment coefficient
C_{M0} = steady moment coefficient at density ρ_1
C_p = pressure coefficient, $\Delta p/(\rho_1 U^2/2)$
c = airfoil chord
F_i = Fourier transform of potential
k = Fourier transform variable
L = half-width of low density strip
p = perturbation pressure
U = undisturbed freestream velocity
v = local velocity normal to airfoil
x = horizontal coordinate
y = vertical coordinate
α = airfoil angle of attack
β_1 = $(\rho_1 - \rho_2)/(\rho_1 + \rho_2)$
β_2 = $(\rho_2 - \rho_3)/(\rho_2 + \rho_3)$
Γ_0 = circulation of basic vortex
γ = vorticity distribution on airfoil
γ_0 = steady-state vorticity distribution on airfoil
$\gamma(y)$ = vorticity on density interface
Δp = local pressure difference across airfoil
η = vertical coordinate
ϑ = angle of density interface
λ = position of density strip midpoint
ξ = horizontal coordinate
ρ_1 = density upstream of strip
ρ_2 = density of strip
ρ_3 = density downstream of strip
$\varphi_i^{(j)}$ = supplmentary potentials
φ_0 = basic vortex potential

Received 10 December 2002; revision received 22 May 2003; accepted for publication 22 May 2003.

*Richard L. and Dorothy M. Hayman Professor, Emeritus, Mechanical Engineering and Jet Propulsion. Fellow AIAA.

I. Introduction

THE response of an airfoil to a normal or inclined strip of low-density gas as it passes over it is related to the interaction of a fan blade with an inlet flow of nonuniform density[1] or to the response of a turbine airfoil to a hot streak of gas emitted from the primary burner of a gas turbine.[2] Although the interaction of a turbine or compressor airfoil to the passage of a wake from upstream has been investigated in some detail,[3,4] there is a fundamental difference between the mechanism of this process and that ocurring during the interaction with a gas strip whose density differs from that of the main stream. For the wake interaction the prescribed velocity distribution of the wake determines the perturbation vorticity field that affects the flow about the airfoil. In a field of nonuniform density, the vorticity, instead of being prescribed, is determined by the interaction of the pressure field of the airfoil with the prescribed density distribution and requires a rather different technique of analysis.

When the density variations are large, that is, not of perturbation order, the analysis is simplified considerably if they occur as sharp density interfaces, for then the vorticity generated is confined to these interfaces. The response of a thin airfoil to a single plane interface normal to the direction of undisturbed flow was described by Marble.[5] One new feature of this study was the introduction of an "image" principle by which the velocity field induced by the vorticity distributed along the entire interface can be represented by image singularities of suitable strength located at image points in the interface. This analytical technique has been used[6] to extend the solution to a single interface convected at any angle to the freestream. The effect of the oblique angle on the airfoil load distribution and lift and moment variations during passage is substantial and physically quite understandable through reference to the image principle.

Because the density differences are considered to be large, the image principle does not extend to the strip problem in a advantageous manner, essentially because the strip can be considered as two parallel density interfaces and strong density differences preclude superposition. In a manner similar to that employed to develop the

theory for a single density interface, the corresponding solution for a vortex moving in the presence of a pair of plane parallel density interfaces will be developed. Examination of the solution reveals that it consists of an infinite sequence of image vortices, each more remote and of correspondingly weaker strength. Some general characteristics of the solution will be examined including the resulting vorticity distributions on each of the density interfaces. Finally these results will be used to develop the theory of the unsteady motion of a thin airfoil encountering a general low-density strip. Although the density difference enters the problem in a nonlinear manner, it is tempting to think intuitively in terms of the superposition of two much simpler isolated interfaces. Although the accuracy of the results is impared, particularly for narrow strips of very low density, the insight obtained into the mechanisms of the solution is quite valuable.

It must be kept in mind that the results obtained from the model destribed here and those of the technological problem of the "hot streak" will differ in some respects. Unless the flow under consideration contains shocks, the main differences result from the behavior of boundary layers in the presence of the density variations and strong pressure gradients. Such effects are evident from the numerical calculations of Ramer,[7] Wijesinghe,[8] and Wijesinghe et al.[9] It is believed, however, that the essential structure of the flowfield is described with clear physical insight in the analysis described here.

II. Point Vortex Moving Near Two Parallel Density Interfaces

Consider an undisturbed fluid divided by vertical density interfaces into three regions, with the central one, of breadth $2L$, located symmetrically with respect to the y axis (Fig. 1). Let the basic vortex potential be that given by Eq. (1), where it is understood that the position ξ, η of the

$$\varphi_0(x, y; t) = -(\Gamma_0/2\pi)\tan^{-1}[(y-\eta)/(x-\xi)] \tag{1}$$

vortex can be a function of time so that the velocity components of the vortex are $\dot{\xi}$ and $\dot{\eta}$. Following the procedure used in Ref. 5, denote the three supplementary potentials φ_1, φ_2, and φ_3, which, together with the basic potential, Eq. (1), satisfy the conditions on the two interfaces at $x = \pm L$ as well as at $x = \pm\infty$.

The conditions to be satisfied at the density interfaces $x = \pm L$ are first, the continuity of the normal velocity component. This requires

$$\frac{\partial}{\partial x}(\varphi_0 + \varphi_1)_{x=L} = \frac{\partial}{\partial x}(\varphi_0 + \varphi_2)_{x=L}$$

$$\frac{\partial}{\partial x}(\varphi_0 + \varphi_2)_{x=-L} = \frac{\partial}{\partial x}(\varphi_0 + \varphi_3)_{x=-L}$$

Because the basic potential φ_0 is regular at both interfaces, the preceding relations reduce to

$$\frac{\partial\varphi_1}{\partial x}(L, y) = \frac{\partial\varphi_2}{\partial x}(L, y) \tag{2}$$

$$\frac{\partial\varphi_2}{\partial x}(-L, y) = \frac{\partial\varphi_3}{\partial x}(-L, y) \tag{3}$$

The second condition to be satisfied is the continuity of pressure at each interface. Because the velocity field of the medium is of perturbation order, the pressure disturbances are, in general, given by $p = -\rho(\partial\varphi/\partial t)$. As a consequence, the pressure continuity at $x = L$ is ensured by

$$\rho_1\frac{\partial}{\partial t}(\varphi_0 + \varphi_1)_{x=L} = \rho_2\frac{\partial}{\partial t}(\varphi_0 + \varphi_2)_{x=L}$$

or

$$\rho_1\frac{\partial\varphi_1}{\partial t} - \rho_2\frac{\partial\varphi_2}{\partial t} = (\rho_2 - \rho_1)\frac{\partial\varphi_0}{\partial t} \tag{4}$$

at $x = L$ and similarly at $x = -L$,

$$\rho_2\frac{\partial\varphi_2}{\partial t} - \rho_3\frac{\partial\varphi_3}{\partial t} = (\rho_3 - \rho_2)\frac{\partial\varphi_0}{\partial t} \tag{5}$$

It is most direct to formulate the problem through Fourier transforms with respect to y. Call

$$F_i(x, k) = \frac{1}{\sqrt{2\pi}}\int_{-\infty}^{\infty}\varphi_j(x, y)e^{-iky}\,dy \tag{6}$$

and its inverse

$$\varphi_i(x, y) = \frac{1}{\sqrt{2\pi}}\int_{-\infty}^{\infty}F_j(x, k)e^{iky}\,dk \tag{7}$$

Because the potentials $\varphi_j(x, y)$ are harmonic functions, the transforms can, with consideration for the boundary conditions to be satisfied at $x = \pm\infty$, be written as

$$F_1 = A_1(k)e^{-|k|x} \tag{8}$$

$$F_2 = A_2(k)e^{-|k|x} + B_2(k)e^{|k|x} \tag{9}$$

$$F_3 = B_3(k)e^{|k|x} \tag{10}$$

The functions $A_1(k)$, $A_2(k)$, $B_2(k)$, and $B_3(k)$ are determined by transforms of the matching conditions, Eqs. (2–5), at the two density interfaces.

The complete solution requires supplementary potentials describing the flow in each of the three regions when the basic vortex is located each of the three regions. Thus, there are a total of nine representations of the potential, which will be designated $\varphi_i^{(j)}$, $i, j = 1, 2, 3$. The index j represents the location of the vortex and i the region in which the flow is being described. There is a corresponding structure of their Fourier transforms $F_i^{(j)}$. Details of this analysis are given in the Appendix.

The solution for the transform $F_1^{(1)}$ of supplementary potential $\varphi_1^{(1)}$, valid for $\xi > 0$ and $k > 0$, takes the following form [see

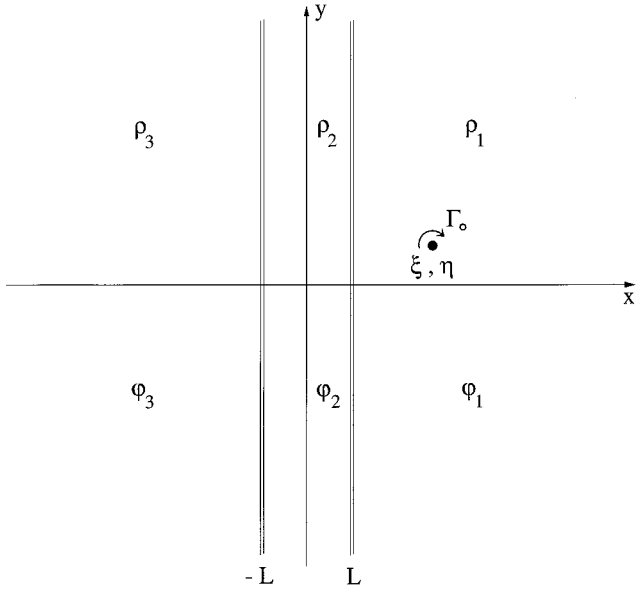

Fig. 1 Basic vortex of circulation Γ_0 moving near a normal strip of width $2L$ and density $\rho_2/\rho_1 = 0.5$.

Appendix, Eq. (A17)] and will allow a physical interpretation of structure of the complete solution:

$$\frac{\partial F_1^{(1)}}{\partial t} = \frac{1}{1+\beta_1\beta_2 e^{-4kL}}\left\{\left(\frac{i\Gamma_0}{2\sqrt{2\pi}}\right)(\dot{\xi}+i\dot{\eta}) \times\left[-\beta_1 e^{-k(x+\xi-2L+i\eta)}-\beta_2 e^{-k(x+\xi+2L+i\eta)}\right]\right\} \tag{11}$$

In this expression β_1 and β_2 are the strengths of the two density interfaces

$$\beta_1 = \frac{\rho_1-\rho_2}{\rho_1+\rho_2}, \qquad \beta_2 = \frac{\rho_2-\rho_3}{\rho_2+\rho_3} \tag{12}$$

The expression within the brace represents the image vortices of strengths $\beta_1\Gamma_0$ and $\beta_2\Gamma_0$ as if the two interfaces were isolated. Together they do not represent the solution because the field of each violates the matching conditions on the interface that generates the other. It is, of course, the factor preceding the brace that completes the solution. Writing this factor as the series

$$\frac{1}{1+\beta_1\beta_2 e^{-4kL}} = \sum_{n=0}^{\infty}(-\beta_1\beta_2)^n e^{-4nkL} \tag{13}$$

allows the complete expression for $\partial F_1^{(1)}/\partial t$ to be written, for $\xi > 0$ and $k > 0$,

$$\frac{\partial F_1^{(1)}}{\partial t} = \left(\frac{i\Gamma_0}{2\sqrt{2\pi}}\right)(\dot{\xi}+i\dot{\eta})\left\{-\beta_1\sum_{n=0}^{\infty}(-\beta_1\beta_2)^n e^{-k[x+\xi+(4n-2)L+i\eta]} - \beta_2\sum_{n=0}^{\infty}(-\beta_1\beta_2)^n e^{-k[x+\xi+(4n+2)L+i\eta]}\right\} \tag{14}$$

in which form this transformation can be inverted and integrated with respect to time. The resulting potential is

$$\varphi_1^{(1)} = \frac{\Gamma_0}{2\pi}\left\{-\beta_1\sum_{n=0}^{\infty}(-\beta_1\beta_2)^n \tan^{-1}\left[\frac{y-\eta}{x+\xi+(4n-2)L}\right] - \beta_2\sum_{n=0}^{\infty}(-\beta_1\beta_2)^n \tan^{-1}\left[\frac{y-\eta}{x+\xi+(4n+2)L}\right]\right\} \tag{15}$$

The first term ($n = 0$) in each series represents the simple reflections just given by the bracketed expressions in Eq. (11). The terms for $n > 0$ represent the multiple reflections in the form of strengths $\beta_1(-\beta_1\beta_2)^n\Gamma_0$ and $\beta_2(-\beta_1\beta_2)^n\Gamma_0$ located, respectively, at positions $-\xi-(4n-2)L$ and $-\xi-(4n+2)L$. Because the values of $|\beta_1|$ and $|\beta_2|$ are less than unity and because the successive images are more remote, the representation usually converges quite rapidly. It is a matter of detailed calculation to obtain explicit representations for $F_i^{(j)}$ and the corresponding Fourier inversions giving $\varphi_i^{(j)}$ valid for the three possible locations of the basic vortex $\xi > L$, $-L < \xi < L$, and $\xi < -L$.

To this point, the density in each of the three regions has been left arbitrary so that the nature of the interactions similar to those discussed in the preceding paragraph can be identified. For the problem of the low-density strip, however, the densities ρ_3 and ρ_1 are equal with the result that $\beta_1 = -\beta_3 \equiv \beta$. The expressions for the supplementary velocity potentials are correspondingly simplified, and the complete set is given in the Appendix.

The potentials given by Eqs. (A16–A24) of the Appendix allow calculation of upwash velocities induced on an airfoil, and, consequently, unsteady airfoil theory can be extended correspondingly. When the airfoil is aligned with the horizontal axis, the Green's function is simply calculated from the appropriate choice of $\partial\varphi_i^{(j)}/\partial y$ and the results entered into the integral equation for the modified vorticity distribution γ_1. When the strip is inclined (Fig. 2), the most direct approach is to rotate the airfoil until the strip returns to the position (Fig. 3), where the preceding solution holds. The upwash calculation then requires the resolution of both velocity components

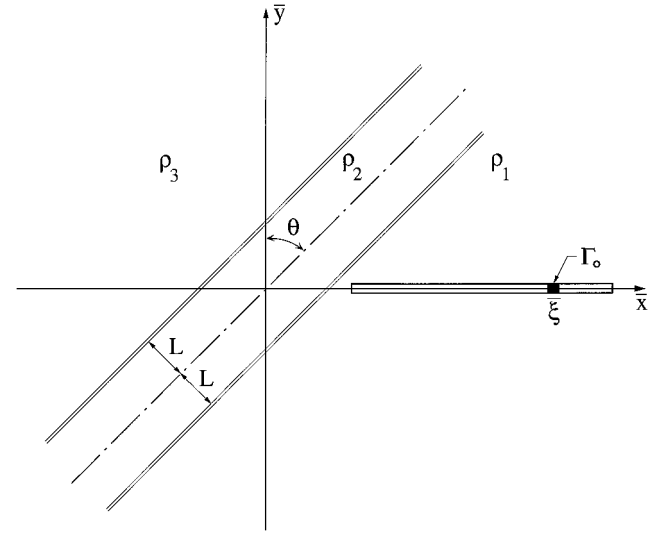

Fig. 2 Configuration of airfoil vortex element near inclined low-density strip of width 2*L*.

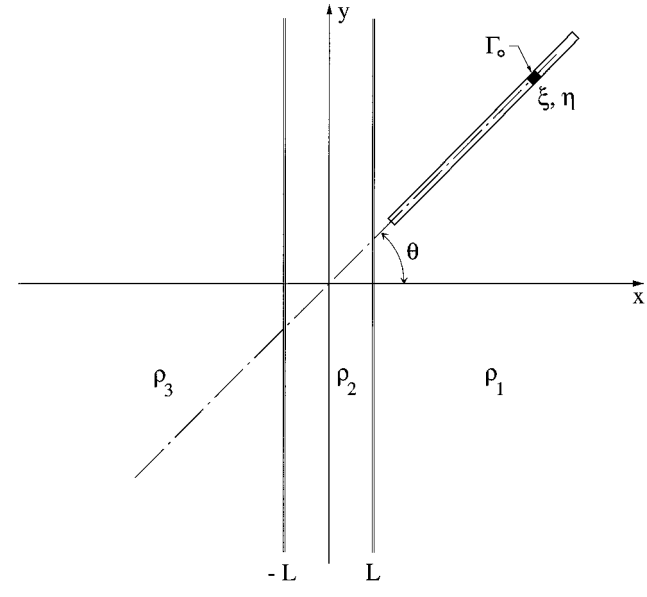

Fig. 3 Configuration of Fig. 2 rotated to place low-density strip in position of Fig. 1.

normal to the airfoil surface, from which the appropriate Green's function is easily extracted. The determination of the modified vorticity distribution and the airfoil response then proceeds as detailed in Refs. 5 and 6. But prior to presenting these results, it is interesting to examine the additional features, over those found with the single interface, that occur when the strip interacts with a single vortex.

III. Velocities Induced in Airfoil Plane

Figure 4 shows a normal strip of density ratio 0.5 and width $L/(c/2) = 0.3$. The vertical velocity induced by a vortex of circulation Γ_0 is plotted in the dimensionless form $\pi cv/\Gamma_0$ for three different positions of the vortex along the horizontal axis. Consider first the vortex at $x/(c/2) = 0.4$, that is, to the right of the interface at $x = L$; the corresponding vertical velocity is shown in solid. As an approximation, treat the interaction of this vortex with each density interface as if it were isolated, that is, as if the principle of images developed for a single interface holds independently for each interface. For the region $x > L$ the vertical velocity is induced largely by the vortex image reflected in the interface at $x = L$. The resulting induced velocity is very close to that found for the isolated density interface. The interface at $x = -L$ is too remote to have much

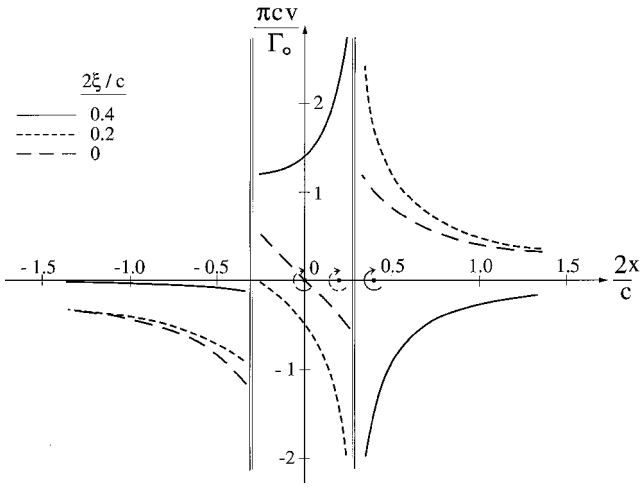

Fig. 4 Vertical velocity induced by normal low-density strip with the basic vortex in three different positions: $L/(c/2) = 0.3$, $\rho_2/\rho_1 = 0.5$, and $\vartheta = 0$.

influence; the relevant image vortex is situated at $x/(c/2) = -1.0$. For the flow within the strip itself, that is, for $-L < x < L$, the relevant vortex image in the right-hand interface lies at $x/(c/2) = 0.4$, and the vertical velocity (the solid curve in this region) is now very slightly influenced by the induction associated with the left-hand interface; the values of the induced velocity are essentially determined by the image vortex at $x/(c/2) = 0.4$. To the left of the interface at $x = -L$, the situation is substantially changed. The relevant image in the right-hand interface remains at $x/(c/2) = 0.4$, but the relevant image in the left-hand interface has now moved also to $x/(c/2) = 0.4$, the position of the basic vortex. Furthermore, because the strength of the left-hand interface is $-\beta\Gamma_0$ the image is of opposite sign. Thus the two images that have moved to the point $x/(c/2) = 0.4$ cancel each other, and the only remaining induction for $x/(c/2) < 0.3$ is the error we have made in assuming the the two density interfaces act as if they were independent. The vertical velocity represented by the solid curve left of the strip in a measure of contribution of nonlinearity in the present instance. To a reasonable degree of accuracy, therefore, it can be said that a basic vortex to the right of the strip does not communicate to the left-hand side of the strip.

Consider now the basic vortex located at $x/(c/2) = 0.2$, just to the left of the right-hand density interface; its induced vertical velocities are shown in the short dashes. For the induction in the region $x/(c/2) > 0.3$, the relevant image is at $x/(c/2) = 0.2$, but because the basic vortex is now viewing this interface from the side opposite that of the basic vortex considered earlier it appears to be of opposite strength. The image is consequently of opposite sign as the basic vortex, and the velocity induced in the region $x > L$ is as shown and is relatively unaffected by the second, remote, interface. Finally for the region $x/(c/2) < -L/(c/2)$, the image of the basic vortex in the left-hand interface is located at $x/(c/2) = 0.2$, and because the left-hand interface is of strength $-\beta\Gamma_0$ it is of opposite sign as the basic vortex. The image in the right-hand interface is at the point $x/(c/2) = 0.4$, and because the basic vortex views this interface from the left side this image is also of sign opposite to that of the basic vortex. Both of these images then induce vertical velocity components of the same sign and produce the distribution shown in short dashes. When the basic vortex is located at the origin, the problem has a symmetry and because of the sign of the basic vortex produces the antisymmetric set of velocity distributions given by the long dashes.

It is instructive at this point to utilize the results shown in Fig. 4 to compute the vorticity distribution $\pi c\Delta v/\Gamma_0$ on the right-hand interface of the strip induced by the vortex located at the point $\xi/(c/2) = 0.4$ and to compare it with the vorticity that would be induced if the right-hand interface were isolated. In other words, examine the error that would be incurred by considering only the simple vortex image in the right-hand interface. These values are given in Table 1 and show small errors for locations near the axis and significant errors for $y/(c/2) > 0.2$. This suggests that, as will recur subsequently in the paper, judiciously used the simple image rules might allow convenient physical insight into the results of involved calculations.

Table 1 Vorticity distribution $\pi c\Delta v/\Gamma_0$ on density interface

$y/(c/2)$	Single interface	Strip: $L/(c/2) = 0.3$
0	6.895	6.740
0.1	3.560	3.340
0.2	1.556	1.340
0.3	0.883	0.674
0.4	0.600	0.400
0.5	0.455	0.264

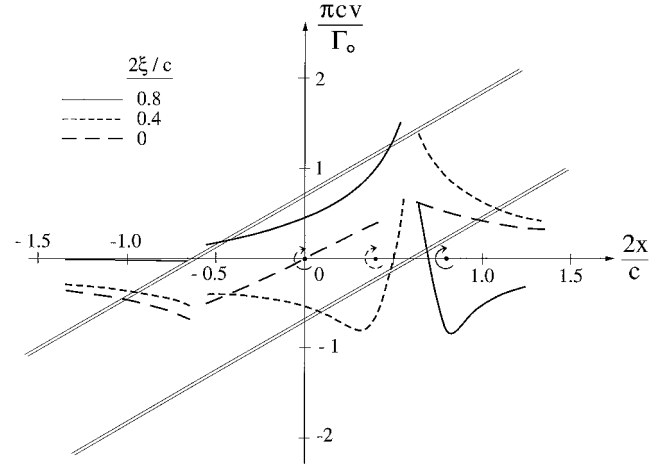

Fig. 5 Vertical velocity induced by inclined low-density strip with the basic vortex in three different positions: $L/(c/2) = 0.3$, $\rho_2/\rho_1 = 0.5$, and $\vartheta = 60$ deg.

Figure 5 shows the corresponding induction patterns for an inclined strip of thickness of $2L$. Note that the region of intersection with the plane of the airfoil is consequently longer, $2L/\cos\vartheta$, a fact that will have some influence on pressure coefficients and on the lift and moment coefficients. These patterns can be analyzed again utilizing the image rules and accounting for peculiarities introduced by the inclination, discussed in Ref. 6.

For the basic vortex at $x/(c/2) = 0.8$, on the right side of the strip the vertical velocity on the right side of the strip is induced by its image within the strip. This velocity is shown by the solid curve and resembles closely the corresponding distribution shown in Fig. 8 in Ref. 6 for the single inclined interface. As expected, this result is caused primarily by the right-hand interface of the strip. The vertical velocity for the region within the strip is induced largely by the image located at the position of the basic vortex and is shown as the solid curve; again, comparison with results in Fig. 8 in Ref. 6 confirm that the main induction comes from the right-hand interface of the strip. Again, the region to the left of the strip is largely isolated from from the basic vortex to the right of the strip and for the same reason discussed with regard to the normal strip (Fig. 4). When the basic vortex is located at $x/(c/2) = 0.5$, the induced vertical velocity is given by curves in short dashes. The velocity to the right of the strip is induced by the image at the basic vortex itself and hence is scarcely influenced by the inclination of the strip. Between the two interfaces, within the strip the principal induction comes from the image in the right-hand interface, which, because the basic vortex views this interface from the rear, is changed in sign and consequently produces the shown distribution. To the left of the strip, the principal induction comes from the image in the left-hand interface and, accounting for the sign of the interface strength, produces the distribution of the expected shape. Finally, the basic vortex at the origin induces velocities, shown as the long

dashes, upstream and downstream of the strip by the vortex images at the origin because of both upstream and downstream interfaces and because the right-hand interface is being viewed from the left, both images are of the same sign. Consequently, the induced velocities are antisymmetric and of equal magnitude. Within the strip the velocity pattern is not what might initially be expected. The induction comes from the two images, one to the right of the strip and one to the left. Again, because of the way the basic vortex views each interface the sense of each vortex is counterclockwise. Because the image that lies to the right of the strip induces velocities that are nearly horizontal in the region $0 < x/(c/2) < 0.6$, the image that lies to the left of the strip is responsible for the vertical velocity in this region. The sign and position of this image vortex produce the unexpected vertical velocity pattern within the right-hand portion of the strip. This reasoning can be repeated for the vertical velocity in the left-hand side of the strip in which case the image vortex to the right of the strip is largely responsible.

IV. Application to Flat-Plate Airfoil Moving Through a Strip

Calculation of the loading, lift, and moment coefficients for a thin airfoil requires first the determination of the vorticity distribution $\gamma_1(\xi)$ induced by the density nonuniformities and the wake produced by the nonsteady motion. This is accomplished by solution of Eq. (19) in Ref. 6 as it was for the case of a single density interface. To carry this out requires the known undisturbed vorticity distribution $\gamma_0(\xi)$ for the airfoil in steady motion through a field of uniform density and the vertical velocities induced by the distributed vorticity generated by the presence of the nonuniform density. The former is assumed known for any airfoil under consideration. The vertical velocities induced by a low-density strip are calculated from the supplementary potentials described earlier and tabulated in detail as Eqs. (A20–A28) in the Appendix. These are employed similarly to Eqs. (8–12) in Ref. 6, which allowed calculation of the induction for the single interface. Whereas the Green's function Q for the single interface required four different representations depending upon the location ξ of the vortex element and the location x of the point where the vertical velocity is being calculated, the Green's function for the strip requires nine different representations. For example, when the vortex element is in region 1 as shown in Fig. 4 for the vortex at $2\xi/c = 0.4$, the induced velocities in region 1 can be calculated using Eq. (A20), and consequently the representation of Q is given by

$$\frac{2\pi}{\Gamma_0}\frac{\partial \varphi_1^{(1)}}{\partial y} = -\sum_{n=0}^{\infty} \beta^{2n+1} \frac{4L}{(x+\xi+4nL)^2 - (2L)^2} \tag{16}$$

where the derivative has been evaluated at $y = \eta = 0$.

In only one respect is this procedure more involved than for the single interface. When treating an inclined strip, the potentials $\varphi_i^{(j)}$ as given in Eqs. (A20–A28) are valid in the x–y reference frame shown in Fig. 3. Consequently, the velocity normal to the airfoil must be resolved from the individual components. Then by interpreting these in the orientation of Fig. 2, the computational procedure of Ref. 6 is directly applicable.

To illustrate the application of the foregoing analysis, consider a flat-plate airfoil of chord c and angle of attack α for which the basic vorticity distribution is

$$\gamma_0(\xi) = 2U\alpha\sqrt{\frac{1-[\xi(c/2)]}{1+[\xi(c/2)]}} \tag{17}$$

Figures 6a–6f show the vorticity distribution on the airfoil resulting from the passage of a normal density strip $\vartheta = 0$, of breadth $L/(c/2) = 0.4$, and of density ratio $\rho_2/\rho_1 = 0.5$, over the airfoil. The variable $\lambda/(c/2)$ gives the position of the centerline of the strip with respect to the midpoint of the airfoil. In Fig. 6a for the value of $\lambda/(c/2) = -1.6$, the leading edge of the strip is at a value of $\xi/(c/2) = -1.2$, just ahead of the leading edge of the airfoil. If the problem involved only the single density interface at this point, the vorticity distribution would be that given in Fig. 10a of Ref. 6, the difference being the influence of the finite strip. This comparison shows that the interface that terminates the strip, which lies at $\xi/(c/2) = -2.0$, has very little influence when the strip is in this position. In Fig. 6b, however, where $\lambda/(c/2) = -1.1$, the right edge of the strip has moved to the point $\xi/(c/2) = -0.7$ and comparison with the vorticity distribution for the single interface at the same position, given in Fig. 10b of Ref. 6, shows the beginning of the influence of the finite strip. Later in its passage over the airfoil, for $\lambda/(c/2) = -0.3$ and especially for $\lambda/(c/2) = 0.3$, the vorticity induced by the two interfaces of opposite sign is particularly evident. By the time the $\lambda/(c/2) = 1.6$ the rear interface of the strip has moved to $\xi/(c/2) = 1.2$ off trailing edge of the airfoil and the induction introduced by the strip is decreasing.

With the vorticity distribution known as a function of the position of the strip, the chordwise distribution of pressure difference can be calculated directly by integration of the streamwise equation of motion in the manner described by Eqs. (20–23) of Ref. 6. From these results the lift and moment coefficents can be calculated as a function of the position of the low-density strip as it passes over the airfoil. Figures 7a and 8a give these values for a normal strip of half-width $L/(c/2) = 0.4$ and density $\rho_2 = 0.5\rho_1$ as a function of λ, the midpoint of the strip. Looking first at the lift coefficients, the first encounter by the right-hand interface behaves very much like that of an isolated interface. It must be kept in mind that right-hand interface arrives at the leading edge of the airfoil when the position of the midpoint $\lambda/(c/2)$ is equal to $-1.0 - L/(c/2)$, which has the value -1.4. Similarly, the left-hand interface encounters the leading edge when $\lambda/(c/2) = -0.6$ and induces the strong response of the lift coefficient in the neighborhood of that point. At this point the entire strip is on the airfoil and remains so until, when $\lambda/(c/2) = 0.6$, the right-hand interface of the strip passes the trailing edge at which point the lift coefficient responds to the adjustment required to satisfy the Kutta condition. Finally the left interface of the strip passes over the trailing edge when $\lambda/(c/2) = 1.4$ and the lift coefficient returns to its undisturbed value. The behavior of the moment coefficient Fig. 8a, which can be understood in a similar fashion, has some significant characteristics that will be discussed subsequently.

As was seen when examining the results for the single interface,[6] the response can be separated into two distinct parts: the interaction of the basic vorticity γ_0 with the nonuniform density field and the effects of the induced vorticity γ_1 and the resulting vortex wake. To determine the former, calculate first the local pressure loading $\Delta p(x)$ by integrating the equation

$$\rho\left(\frac{\partial \gamma}{\partial t} + U\frac{\partial \gamma}{\partial x}\right) = -\frac{\partial \Delta p}{\partial x} \tag{18}$$

from the trailing edge, where $\Delta p = 0$, taking account of the appropriate value of ρ for the region in which integration is being carried out. The integration is particularly straightforward because the basic vorticity γ_0 is independent of time. For example, when the strip of breadth $2L = 0.4c$ is situated so that the strip is entirely on the airfoil, that is, $(c/2 - L) > \lambda > (-c/2 + L)$, the integration of Eq. (18) gives, for $c/2 > x > \lambda + L$,

$$\Delta p(x) = -\rho_1 U \gamma_0(x) \tag{19}$$

For $\lambda + L > x > \lambda - L$,

$$\Delta p(x) = -\rho_2 U \gamma_0(x) - (\rho_1 - \rho_2) U \gamma_0(\lambda + L) \tag{20}$$

and for $\lambda - L > x > -c/2$,

$$\Delta p(x) = -\rho_1 U \gamma_0(x) + (\rho_1 - \rho_2) U \gamma_0(\lambda - L) - (\rho_1 - \rho_2) U \gamma_0(\lambda + L) \tag{21}$$

With these relations known the lift coefficient and the moment coefficient can be calculated by chordwise integration of the loading and the moment of the loading respectively. The expressions

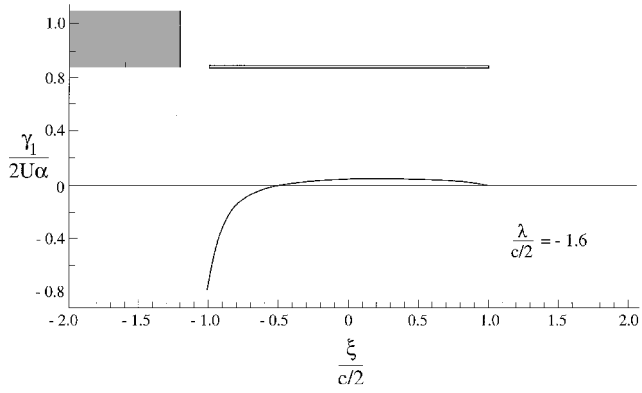

a) $\gamma/(c/2) = -1.6$

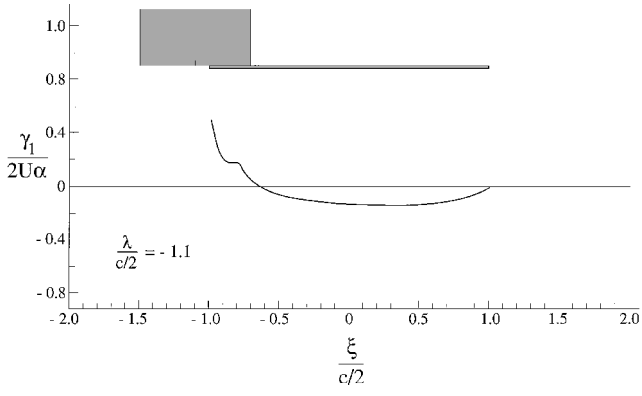

b) $\gamma/(c/2) = -1.1$

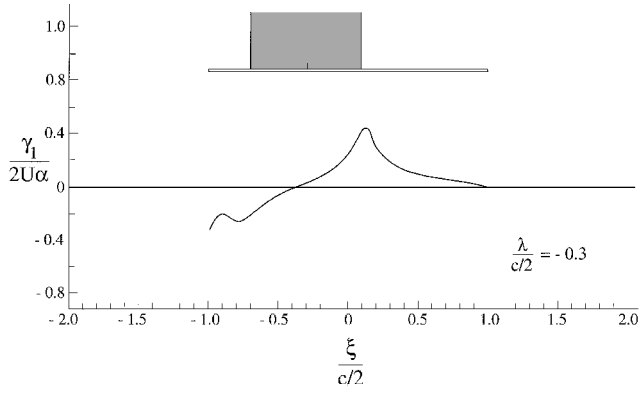

c) $\gamma/(c/2) = -0.3$

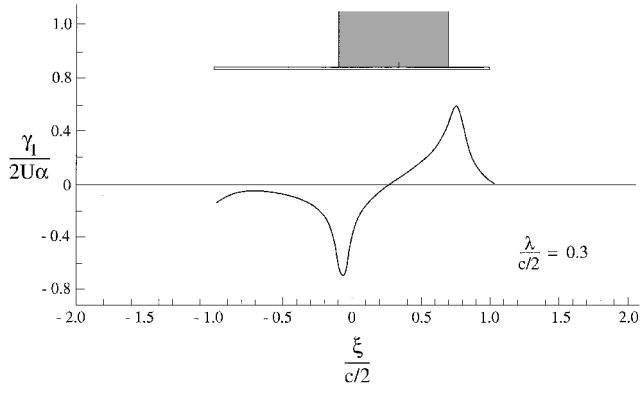

d) $\gamma/(c/2) = 0.3$

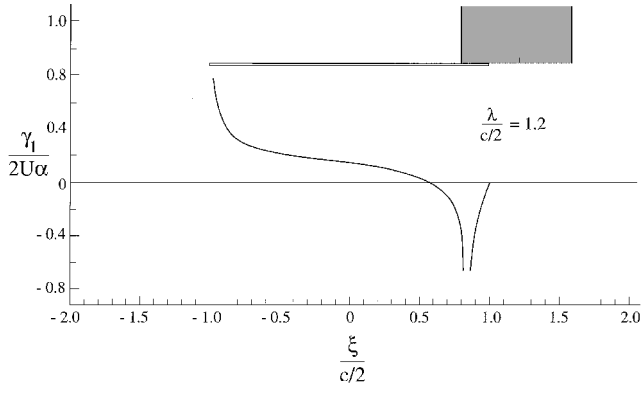

e) $\gamma/(c/2) = 1.2$

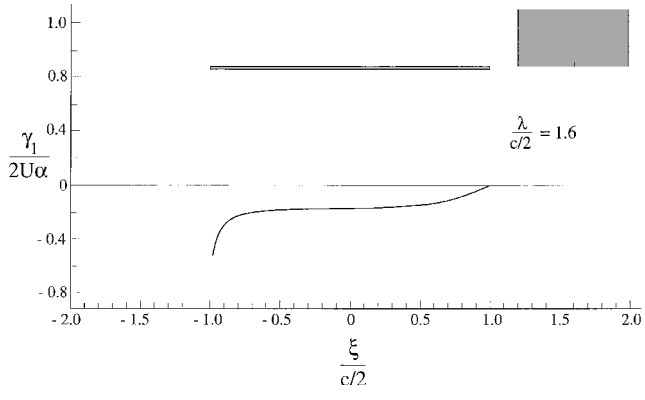

f) $\gamma/(c/2) = 1.6$

Fig. 6 Vorticity distribution $\gamma_1/2U\alpha$ on flat-plate airfoil passing through low-density strip: $L/(c/2) = 0.4$, $\rho_2/\rho_1 = 0.5$, and $\vartheta = 0$.

for these are

$$C_L = 2\pi\alpha\left\{1 - \frac{1}{\pi}\left(1 - \frac{\rho_2}{\rho_1}\right)\left[\cos^{-1}\left(\frac{\lambda - L}{c/2}\right) - \cos^{-1}\left(\frac{\lambda + L}{c/2}\right)\right]\right\} \tag{22}$$

$$C_M = -\frac{\pi}{2}\alpha\left\{1 - \frac{1}{\pi}\left(1 - \frac{\rho_2}{\rho_1}\right)\left[\cos^{-1}\left(\frac{\lambda - L}{c/2}\right) - \cos^{-1}\left(\frac{\lambda + L}{c/2}\right) - \sqrt{1 - \left(\frac{\lambda - L}{c/2}\right)^2} + \sqrt{1 - \left(\frac{\lambda + L}{c/2}\right)^2}\right]\right\} \tag{23}$$

where in each expression the factor preceeding the brace is the steady-state lift and moment coefficient, respectively. The values of the coefficent ratios calculated from these expressions are shown as circles in Figs. 8a and 9a for the range $-0.6 < \lambda/(c/2) < 0.6$. The circled points outside this range are calculated by analysis similar to the preceding for the cases where either the right or left interfaces lie off the airfoil. In fact, the situation in these cases is exactly that for a single interface, and Eqs. (29) and (30) of Ref. 6 can be applied. The differences between the circled points and the solid curve then are the contributions of induction from the vorticity distribution on the interfaces, the vortex wake, and the virtual mass. These assume particular importance when one of the interfaces is passing over the leading or trailing edge of the airfoil.

A set of results is shown in Figs. 7b and 8b for a strip of density ratio $\rho_2/\rho_1 = 0.5$, normal to the flow but with $L/(c/2) = 0.8$. The most significant differences from the results given in Figs. 7a and 8a are in the central section caused by the shorter period where both interfaces are on the airfoil. This difference is even more evident in the results for the strip shown in Figs. 7c and 8c, where $L/(c/2) = 1.2$. In this example there is an interval within which the strip completely covers the airfoil. Consequently, in this interval $0.2 \geq \xi/(c/2) \geq -0.2$ the steady-state values of the lift and moment coefficients are reached.

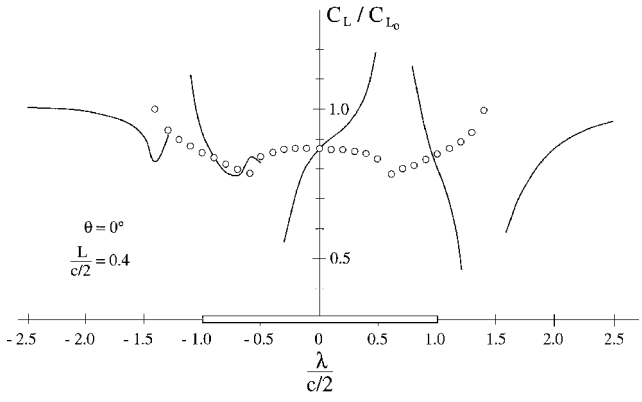

a) $L/(c/2) = 0.4$

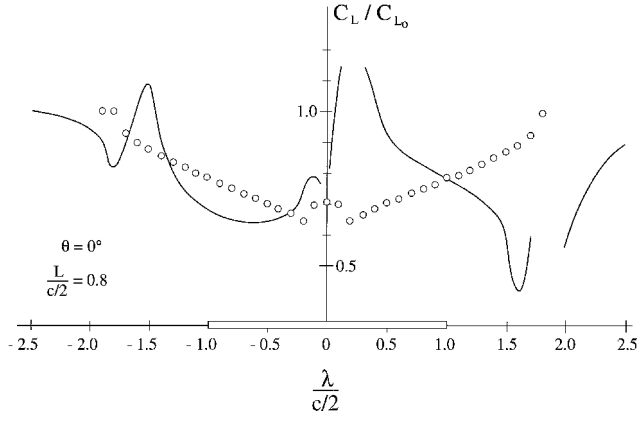

b) $L/(c/2) = 0.8$

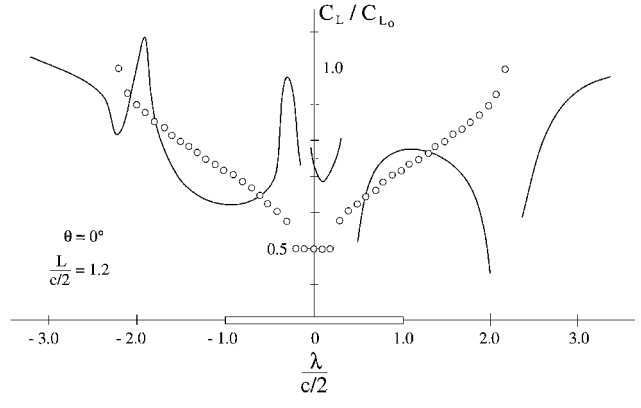

c) $L/(c/2) = 1.2$

Fig. 7 Response of lift coefficient for flat-plate airfoil passing through low-density strip: $\vartheta = 0$ and $\rho_2/\rho_1 = 0.5$.

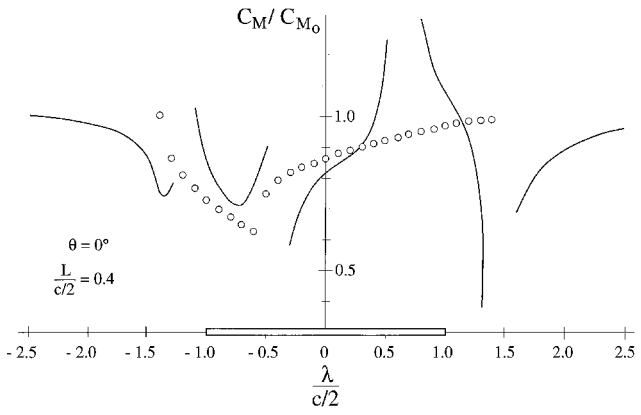

a) $L/(c/2) = 0.4$

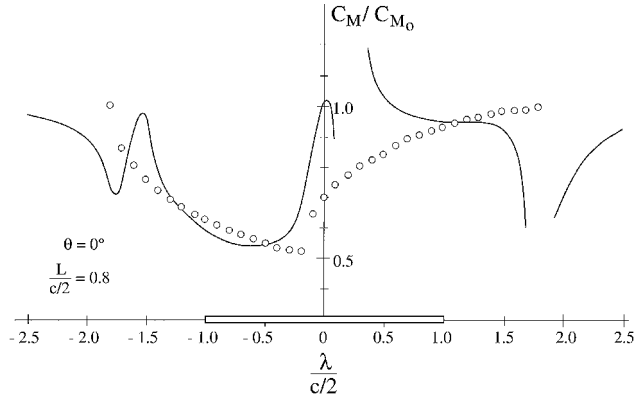

b) $L/(c/2) = 0.8$

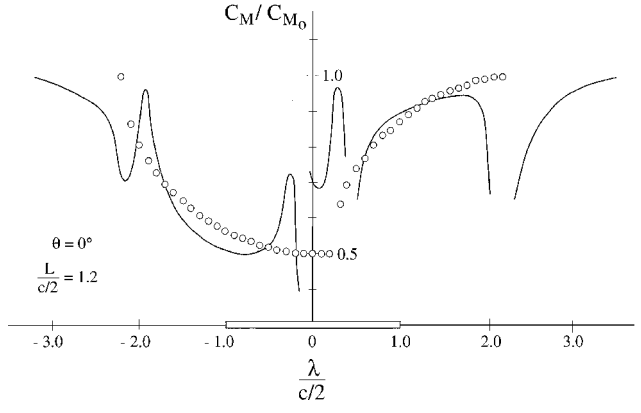

c) $L/(c/2) = 1.2$

Fig. 8 Response of moment coefficient for flat-plate airfoil passing through low-density strip: $\vartheta = 0$ and $\rho_2/\rho_1 = 0.5$.

A corresponding set of lift and moment coefficients are shown in Figs. 9 and 10 for the low-density strip inclined at an angle of 60 deg to the vertical. It must be recalled that the inclined strip presents a projection of $2L/\cos\vartheta$ on the plane of the airfoil, which for the results shown in Figs. 9b and 10b is 1.6 c, twice that of the corresponding normal strip. One consequence of this is a major change in the timing of the impulses from that for the same low-density strip aligned normal to the flow, as shown in Figs. 7b and 8b. Referring now to lift-coefficient response shown in Fig. 9b, the right interface of the inclined strip passes over the leading edge when $\lambda/(c/2) = -2.6$ and consequently not shown. However the right interface passes off the trailing edge when $\lambda/(c/2) = -0.6$, which accounts for the impulse at that point. The left interface crosses the leading edge when $\lambda/(c/2) = 0.6$, and the associated lift impulse occurs somewhat later as has been observed generally when an interface passes the leading edge, even when only a single interface is involved as, for example, Fig. 9a of Ref. 6.

When the strip is narrower, as in Fig. 9a where $L/(c/2) = 0.4$, the the origins of the lift pulses are more directly recognized. The right interface of this inclined strip crosses the leading edge when $\lambda/(c/2) = -1.8$, the associated pulse lagging slightly. The left interface crosses the leading edge when $\lambda/(c/2) = -0.2$ and is closely followed the pulse associated with the right-hand interface leaving the trailing edge when $\lambda/(c/2) = 0.2$. Finally the left-hand interface leaves the trailing edge when $\lambda/(c/2) = 1.8$. The response of the moment coefficients (Figs. 10a and 10b) can be analyzed in a similar manner.

Finally one can examine the contribution of the direct interaction of the basic airfoil vorticity γ_0 with the nonuniform density field. Referring to the analysis beginning with Eq. (18) for the normal strip, recall that integration of this equation involves only conditions on the horizontal axis and the upper and lower surfaces of the airfoil and not in the remainder of the field. Thus, only the properties at the intersection of the strip with the airfoil enter the calculation. As a

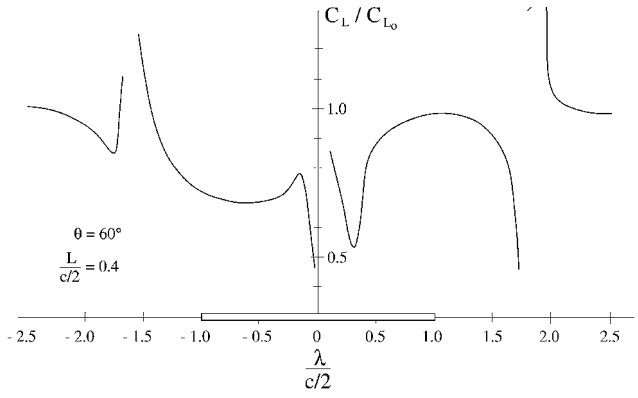

a) $L/(c/2) = 0.4$

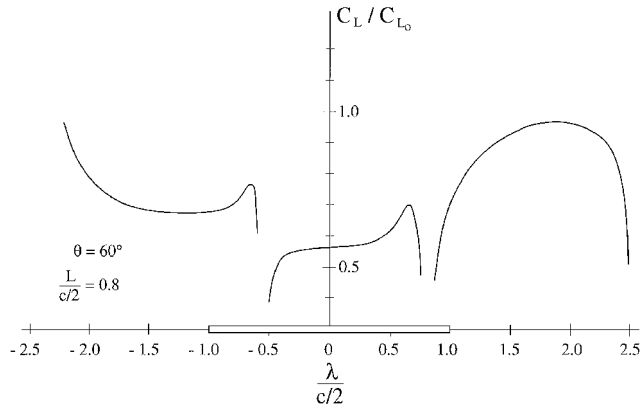

b) $L/(c/2) = 0.8$

Fig. 9 Response of lift coefficient for flat-plate airfoil passing through inclined low-density strip: $\vartheta = 60$ deg and $\rho_2/\rho_1 = 0.5$.

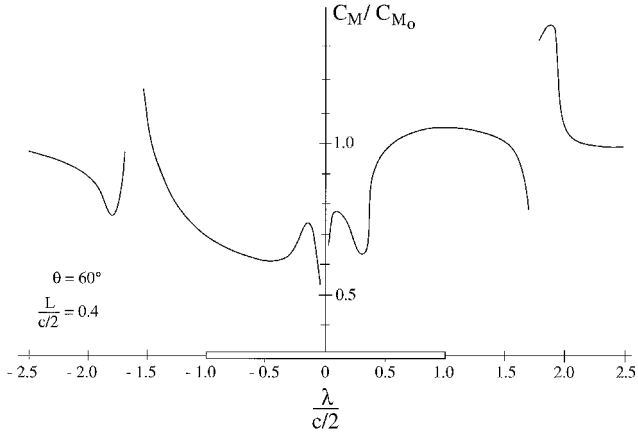

a) $L/(c/2) = 0.4$

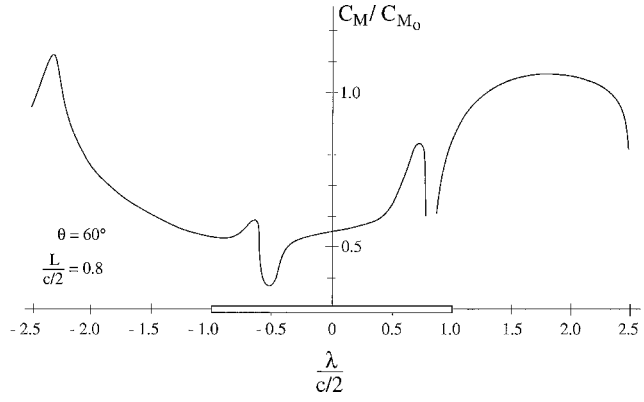

b) $L/(c/2) = 0.8$

Fig. 10 Response of moment coefficient for flat-plate airfoil passing through inclined low-density strip: $\vartheta = 60$ deg and $\rho_2/\rho_1 = 0.5$.

consequence, expressions given in Eqs. (22) and (23) can be used for the inclined interface provided only that the half-width L of the strip is replaced with $L/\cos\vartheta$, its projected value. Therefore the circles appearing in Figs. 7b and 8b for the normal strip of $L/(c/2) = 0.8$ are the appropriate values for the 60-deg inclined strip shown in Figs. 9a and 10a for which $L/(c/2) = 0.4$.

Appendix: Solution for Supplementary Potentials

Call the Fourier transforms of the potentials

$$F_i(x,k) = \frac{1}{\sqrt{2\pi}} \int_{-\infty}^{\infty} \varphi_i(x,y) e^{-iky}\, dy \tag{A1}$$

and their inverse transforms

$$\varphi_i(x,k) = \frac{1}{\sqrt{2\pi}} \int_{-\infty}^{\infty} F_i(x,y) e^{iky}\, dk \tag{A2}$$

Because the potentials $\varphi_i(x,y)$ are harmonic functions, the transforms can, with consideration for the boundary conditions to be satisfied at $x = \pm\infty$, be written as

$$F_1 = A_1(k) e^{-|k|x} \tag{A3}$$

$$F_2 = A_2(k) e^{-|k|x} + B_2(k) e^{|k|x} \tag{A4}$$

$$F_3 = B_3(k) e^{|k|x} \tag{A5}$$

It must be remembered that the solution requires potentials describing the flow in each of them three regions when the basic vortex is located each of the three regions. Thus there are a total of nine representations of the potential that we designate $\varphi_i^{(j)}$, $i, j = 1, 2, 3$. The index j represents the location of the vortex and i the region in which the flow is being described. There is a corresponding structure of their Fourier transforms $F_i^{(j)}$.

The functions $A_1(k)$, $A_2(k)$, $B_2(k)$, and $B_3(k)$ are determined by the matching conditions, Eqs. (2–5), at the two density interfaces. The transforms of Eqs. (2) and (3) give the relations

$$-|k|A_1 e^{-|k|L} = -|k|A_2 e^{-|k|L} + |k|B_2 e^{|k|L} \tag{A6}$$

$$-|k|A_2 e^{|k|L} + |k|B_2 e^{-|k|L} = |k|B_3 e^{-|k|L} \tag{A7}$$

Equations (4) and (5), conditions assuring the continuity of pressure across each of the interfaces, give two more relations:

$$\rho_1 \frac{\partial A_1}{\partial t} e^{-|k|L} - \rho_2 \left(\frac{\partial A_2}{\partial t} e^{-|k|L} + \frac{\partial B_2}{\partial t} e^{|k|L} \right) = (\rho_2 - \rho_1) \frac{\partial F_0}{\partial t}(L,k) \tag{A8}$$

$$\rho_2 \left(\frac{\partial A_2}{\partial t} e^{|k|L} + \frac{\partial B_2}{\partial t} e^{-|k|L} \right) - \rho_3 \frac{\partial B_3}{\partial t} e^{-|k|L} = (\rho_3 - \rho_2) \frac{\partial F_0}{\partial t}(-L,k) \tag{A9}$$

These four relations can be solved for values of $\partial A_1/\partial t$, $\partial A_2/\partial t$, $\partial B_2/\partial t$, $\partial B_3/\partial t$ and subsequently for expressions for the Fourier transforms

$$\frac{\partial F_1}{\partial t} = \frac{1}{1 + \beta_1\beta_2 e^{-4|k|L}} \left\{ -\beta_1 D_1 e^{-|k|x} + \beta_2 D_2 e^{-|k|(x+2L)} \right\} \tag{A10}$$

$$\frac{\partial F_2}{\partial t} = \frac{1}{1 + \beta_1\beta_2 e^{-4|k|L}} \left\{ \beta_2 D_2 e^{-|k|(x+2L)} + \beta_1 D_1 e^{|k|(x-2L)} \right\} \tag{A11}$$

$$\frac{\partial F_3}{\partial t} = \frac{1}{1+\beta_1\beta_2 e^{-4|k|L}}\left\{-\beta_2 D_2 e^{|k|x} + \beta_1 D_1 e^{|k|(x-2L)}\right\} \quad \text{(A12)}$$

in each of the three regions. In these expressions β_1 and β_2 are the strengths of each density interface:

$$\beta_1 = \frac{\rho_1 - \rho_2}{\rho_1 + \rho_2}, \qquad \beta_2 = \frac{\rho_2 - \rho_3}{\rho_2 + \rho_3} \quad \text{(A13)}$$

and D_1 and D_2 are the determinants

$$D_1 = \begin{vmatrix} e^{-|k|L} & -\dfrac{\partial F_0}{\partial t}(L,k) \\ e^{|k|L} & -\beta_2 \dfrac{\partial F_0}{\partial t}(-L,k) \end{vmatrix} \quad \text{(A14)}$$

$$D_2 = \begin{vmatrix} -\beta_1 \dfrac{\partial F_0}{\partial t}(L,k) & -e^{|k|L} \\ -\beta_2 \dfrac{\partial F_0}{\partial t}(-L,k) & e^{-|k|L} \end{vmatrix} \quad \text{(A15)}$$

In these expressions $\partial F_0/\partial t$ is the Fourier transform of the basic vortex potential $\partial\varphi_0/\partial t$, which, from Eq. (1), is

$$\frac{\partial \varphi_0}{\partial t} = \frac{\Gamma_0}{2\pi}\left\{\frac{(x-\xi)\dot{\eta} - (y-\eta)\dot{\xi}}{(x-\xi)^2 + (y-\eta)^2}\right\} \quad \text{(A16)}$$

The results of the transform operation depend upon whether the position of the vortex is greater than or less than the value of x at which the potential is evaluated and further upon the sign of the wave number k. Consequently, four expressions are obtained.

$\xi < x$:

$$\frac{\partial F_0}{\partial t} = i\left(\frac{\Gamma_0}{2\sqrt{2\pi}}\right)(\dot{\xi} - i\dot{\eta})e^{-k(x-\xi+i\eta)}, \qquad k > 0$$

$$\frac{\partial F_0}{\partial t} = -i\left(\frac{\Gamma_0}{2\sqrt{2\pi}}\right)(\dot{\xi} + i\dot{\eta})e^{k(x-\xi-i\eta)}, \qquad k > 0$$

$\xi > x$:

$$\frac{\partial F_0}{\partial t} = i\left(\frac{\Gamma_0}{2\sqrt{2\pi}}\right)(\dot{\xi} + i\dot{\eta})e^{k(x-\xi-i\eta)}, \qquad k > 0$$

$$\frac{\partial F_0}{\partial t} = -i\left(\frac{\Gamma_0}{2\sqrt{2\pi}}\right)(\dot{\xi} - i\dot{\eta})e^{-k(x-\xi+i\eta)}, \qquad k > 0 \quad \text{(A17)}$$

The information is now available to evaluate explicitly the transformed potentials, Eqs. (A10–A12), and to invert them giving the physical supplementary potentials φ_1, φ_2, and φ_3.

The structure of the supplementary potentials can be understood by examining the solution transform F_1 when $\xi > L$ and $k > 0$. From Eq. (A10)

$$\frac{\partial F_1}{\partial t} = \frac{1}{1+\beta_1\beta_2 e^{-4kL}}\left\{-\beta_1 D_1 + \beta_2 e^{-2kL} D_2\right\} e^{-kx} \quad \text{(A18)}$$

Inserting the determinants D_1 and D_2, Eqs. (A14) and (A15), and the appropriate expressions for the $\partial F_0/\partial t$ from Eq. (A17),

$$\frac{\partial F_1}{\partial t} = \frac{1}{1+\beta_1\beta_2 e^{-4kL}}\left\{\left(\frac{i\Gamma_0}{2\sqrt{2\pi}}\right)(\dot{\xi} + i\dot{\eta})\left[-\beta_1 e^{-k(x+\xi-2L+i\eta)} - \beta_2 e^{-k(x+\xi+2L+i\eta)}\right]\right\} \quad \text{(A19)}$$

This result appears as Eq. (11) of the main text.

To this point the density in each of the three regions has been left arbitrary so that the nature of the interactions similar to those discussed in the preceding paragraph can be identified. For the problem of the low-density strip, however, the densities ρ_3 and ρ_1 are equal with the result that $\beta_1 = -\beta_3 \equiv \beta$. The expressions for the supplementary velocity potentials are correspondingly simplified, and the complete set is given next.

Region 1, $\varphi_1^{(j)}$

$\xi > L$:

$$\varphi_1^{(1)} = \frac{\Gamma_0}{2\pi}\sum_{n=0}^{\infty}\beta^{2n+1}\left\{\tan^{-1}\left(\frac{y-\eta}{x+\xi+(4n+2)L}\right) - \tan^{-1}\left(\frac{y-\eta}{x+\xi+(4n-2)L}\right)\right\} \quad \text{(A20)}$$

$-L < \xi < L$:

$$\varphi_1^{(2)} = \frac{\Gamma_0}{2\pi}\sum_{n=0}^{\infty}\beta^{2n+1}\left\{\tan^{-1}\left(\frac{y-\eta}{x-\xi+4nL}\right) - \beta\tan^{-1}\left(\frac{y-\eta}{x-\xi+(4n+2)L}\right) + (1-\beta)\tan^{-1}\left(\frac{y-\eta}{x+\xi+(4n+2)L}\right)\right\} \quad \text{(A21)}$$

$\xi < -L$:

$$\varphi_1^{(3)} = \frac{\Gamma_0}{2\pi}\sum_{n=0}^{\infty}\beta^{2n+1}\left\{\beta\tan^{-1}\left(\frac{y-\eta}{x-\xi+4nL}\right) - \beta\tan^{-1}\left(\frac{y-\eta}{x-\xi+4(n+1)L}\right)\right\} \quad \text{(A22)}$$

Region 2, $\varphi_2^{(j)}$

$\xi > L$:

$$\varphi_2^{(1)} = \frac{\Gamma_0}{2\pi}\sum_{n=0}^{\infty}\beta^{2n+1}\left\{(1+\beta)\tan^{-1}\left(\frac{y-\eta}{x+\xi+(4n+2)L}\right) - \tan^{-1}\left(\frac{y-\eta}{x-\xi-4nL}\right) - \beta\tan^{-1}\left(\frac{y-\eta}{x-\xi-4(n+1)L}\right)\right\} \quad \text{(A23)}$$

$-L < \xi < L$:

$$\varphi_2^{(2)} = \frac{\Gamma_0}{2\pi}\sum_{n=0}^{\infty}\beta^{2n+1}\left\{\tan^{-1}\left(\frac{y-\eta}{x+\xi-(4n+2)L}\right) - \beta\tan^{-1}\left(\frac{y-\eta}{x-\xi-4(n+1)L}\right) + \tan^{-1}\left(\frac{y-\eta}{x+\xi+(4n+2)L}\right) - \beta\tan^{-1}\left(\frac{y-\eta}{x-\xi+4(n+1)L}\right)\right\} \quad \text{(A24)}$$

$\xi < -L$:

$$\varphi_2^{(3)} = \frac{\Gamma_0}{2\pi}\sum_{n=0}^{\infty}\beta^{2n+1}\left\{(1+\beta)\tan^{-1}\left(\frac{y-\eta}{x+\xi-(4n+2)L}\right) - \tan^{-1}\left(\frac{y-\eta}{x-\xi+4nL}\right) - \beta\tan^{-1}\left(\frac{y-\eta}{x-\xi+4(n+1)L}\right)\right\} \quad \text{(A25)}$$

Region 3, $\varphi_3^{(j)}$

$\xi > L$:

$$\varphi_3^{(1)} = \frac{\Gamma_0}{2\pi}\sum_{n=0}^{\infty}\beta^{2n+1}\left\{\beta\tan^{-1}\left(\frac{y-\eta}{x-\xi-4nL}\right) - \beta\tan^{-1}\left(\frac{y-\eta}{x-\xi-4(n+1)L}\right)\right\} \quad \text{(A26)}$$

$-L < \xi < L$:

$$\varphi_3^{(2)} = \frac{\Gamma_0}{2\pi} \sum_{n=0}^{\infty} \beta^{2n+1} \left\{ (1-\beta) \tan^{-1}\left(\frac{y-\eta}{x+\xi-(4n+2)L} \right) - \beta \tan^{-1}\left(\frac{y-\eta}{x-\xi-4(n+1)L} \right) + \tan^{-1}\left(\frac{y-\eta}{x-\xi-4nL} \right) \right\} \tag{A27}$$

$\xi < -L$:

$$\varphi_3^{(3)} = \frac{\Gamma_0}{2\pi} \sum_{n=0}^{\infty} \beta^{2n+1} \left\{ \tan^{-1}\left(\frac{y-\eta}{x+\xi-(4n+2)L} \right) - \tan^{-1}\left(\frac{y-\eta}{x+\xi-(4n-2)L} \right) \right\} \tag{A28}$$

References

[1]Giles, M. B., and Krouthen, B., "Numerical Investigation of Hot Streaks in Turbines," AIAA Paper 88-3015, 1988.

[2]Shang, T., and Epstein, A. H., "Analysis of Hot Streak Effects on Turbine Rotor Heat Load," *Journal of Turbomachinery*, Vol. 119, 1997, pp. 544–553.

[3]Sears, W. R., "Some Aspects of Non-Stationary Airfoil Theory and Its Practical Application," *Journal of the Aeronautical Sciences*, Vol. 8, No. 3, 1941, pp. 104–108.

[4]Kemp, N. H., and Sears, W. R., "The Unsteady Forces due to Viscous Wakes in Turbomachines," *Journal of the Aeronautical Sciences*, Vol. 22, No. 7, 1955, pp. 478–483.

[5]Marble, F. E., "Response of a Thin Airfoil Encountering a Strong Density Discontinuity," *Symposium on Aerodynamics and Aeroacoustics*, edited by K.-Y., Fung, 1993, World Scientific Singapore, pp. 231–255; also *Journal of Fluids Engineering*, Vol. 115, 1993, pp. 580–589.

[6]Marble, F. E., "Thin Airfoil in Fields of Nonuniform Density, Part 1: Single Density Interface," *AIAA Journal*, Vol. 41, No. 11, 2003, pp. 2085–2094.

[7]Ramer, B. E., "Aerodynamic Response of Turbomachinery Blade Rows to Convecting Density Distortions," M.S. Thesis, Dept. of Aeronautics and Astronautics, Massachusetts Inst. of Technology, Cambridge, MA, Jan. 1997.

[8]Wijesinghe, H. S., "Aerodynamic Response of Turbomachinery Blade Rows to Convecting Density Wakes," M.S. Thesis, Dept. of Aeronautics and Astronautics, Massachusetts Inst. of Technology, Cambridge, MA, Sept. 1998.

[9]Wijesinghe, H. S., Tan, C. S., and Covert, E. E., "Aerodynamic Response of Turbomachinery Blade Rows to Convecting Density Wakes," *Journal of Turbomachinery*, Vol. 124, No. 2, 2002, pp. 269–274.

S. K. Aggarwal
Associate Editor